PHYSICAL REVIEW B VOLUME 49, NUMBER 11 15 MARCH 1994-I

Temperature dependence of the near-infrared refractive index of silicon, gallium arsenide, and indium phosphide

J. A. McCaulley,* V. M. Donnelly, M. Vernon, and I. Taha†
AT&T Bell Laboratories, 600 Mountain Avenue, Murray Hill, New Jersey 07974-2070
(Received 30 August 1993)

Infrared laser interferometry was used to measure the temperature dependence, $\beta(T)$, of the refractive index of Si, GaAs, and InP at $\lambda=1.15$, 1.31, 1.53, and 2.39 μm. Semiconductor wafer samples that had been polished on both sides were either heated or cooled while measuring the sample temperature and the transmitted or reflected intensity of an infrared laser beam. The changing optical path length within the material causes alternating constructive and destructive interference between reflections off the front and back surfaces of the wafer. By subtracting the contribution of thermal expansion, $\alpha(T)$, which is small and accurately known, $\beta(T)$ was obtained. Representative values of β (293 K) at 1.53 μm are 5.15×10^{-5} K^{-1}, 6.65×10^{-5} K^{-1}, and 5.95×10^{-5} K^{-1} for Si, GaAs, and InP. Polynomial expressions are presented for Si, GaAs, and InP, yielding values of $\beta(T)$ that are accurate to within $\pm5\%$. $\beta(T)$ increases with increasing temperature and decreases with increasing wavelength. There is a large resonance enhancement of $\beta(T)$ in direct-gap semiconductors as the photon energy $E_{h\nu}$ approaches the band-gap energy E_g. Absolute values and temperature dependences of β calculated from published theory agree reasonably well with the measurements. The extreme accuracy in β needed for interferometric thermometry, however, cannot be met by these theoretical calculations, and so requires the experimental measurements.

I. INTRODUCTION

The refractive index n is an important parameter in determining the usefulness of a material in optical or optoelectronic applications. Consequently, the refractive indices of Si, GaAs, and InP in the infrared have been studied by many researchers. While there is generally good agreement among most of the studies on the values of the room-temperature refractive indices, there are considerable discrepancies in their temperature dependences, especially at high temperature. At some temperatures and wavelengths, no values are available. In many cases, the discrepancies can be attributed to the degree of accuracy in the experimental methods employed. For example, in 1980 Li reviewed the available data on the refractive index of silicon, and recommended that future measurements of $n(\lambda,T)$ employ interference methods and thick-plate samples to improve on the accuracy of the previous measurements.[1]

We have reported the use of infrared laser interferometric thermometry (IRLIT) for measuring the temperature of semiconductor wafers.[2–4] The same technique was later reported by Sankur and Gunning.[5] More recently Saenger and Gupta[6] reported the use of visible laser interferometric thermometry to measure the temperature of insulating substrates, similar to earlier work by Hacman[7] and Bond, Dzioba, and Naguib.[8] In IRLIT a low-power infrared (IR) laser having a photon energy below the band-gap energy of a semiconductor is directed at a wafer of known thickness h that is polished on both sides. Either the reflected or transmitted intensity is measured with a photodiode. As the temperature of the wafer is increased or decreased the optical path length nh within the wafer increases or decreases, causing interference between reflections off the front and back surfaces. The direction of temperature change can be sensed by exploiting variations in wafer thickness,[3,4,9] or by modulating the laser wavelength.[10] Under some conditions, the technique can also be extended to standard wafers that are polished to an optical finish on only one side.[11] We have applied IRLIT to surface science studies[12] and to semiconductor etching and deposition processes.[13–15]

The change of the optical path length in the semiconductor is dominated by the temperature dependence of n,

$$\beta(T)=(1/n)(dn/dT) \tag{1}$$

with a smaller contribution from thermal expansion,

$$\alpha(T)=(1/h)(dh/dT)\ , \tag{2}$$

where h is the sample thickness. Because $\beta(T)$ is poorly known it was necessary to perform calibration experiments to apply IRLIT. We have recently performed an extensive series of calibration experiments on Si, GaAs, and InP using four different laser wavelengths.[16] Substrates containing various concentrations of donors or acceptors were examined.

Because the interferograms are dominated by changes in the refractive index, $\beta(T)$ can be obtained by subtracting the contribution of $\alpha(T)$ from the interferometric data.[3] Since $\alpha(T)$ is small relative to $\beta(T)$, and well known, $\beta(T)$ can be obtained with good accuracy. Saenger and Gupta used this approach to determine β (298 K) for several insulating materials of 632.8 nm.[6] In our earlier report[3] we mentioned that the temperature dependence of the refractive index of Si, GaAs, and InP at 1.15 μm would be reported in a future publication.

0163-1829/94/49(11)/7408(10)/$06.00 ©1994 The American Physical Society

Though these data are a byproduct of our calibration experiments, they are of intrinsic interest for optoelectronic applications of these materials. Furthermore, $\beta(T)$ is needed to apply IRLIT at off-normal angles of incidences because the angle of incidence within the substrate is temperature dependent. Here, we report $\beta(T)$ for Si, GaAs, and InP over wide temperature ranges at wavelengths λ of 1.15, 1.31, 1.53, and 2.39 μm.

II. EXPERIMENT

The intensity of an infrared laser beam transmitted through, or reflected off, a sample of semiconductor wafer was measured as the sample temperature was slowly varied. Figure 1 presents a schematic diagram of the experimental apparatus and the interference geometry of the transmission measurements used above room temperature.

Semiconductor wafers that were polished on both sides were cleaved to obtain ~10 mm×10 mm samples. The samples used in this study are described in Table I. The thickness of each cleaved sample was measured using a micrometer, with an estimated accuracy of ±0.2%. Si and GaAs samples were typically 0.6-mm thick, and InP samples were ~0.3-mm thick. The samples were clamped between two cylindrical blocks of boron nitride (27-mm diam and 16-mm long) with holes (4.7-mm diam) drilled through to enable transmission of the laser beam. The temperature of the sample was measured with either a stainless-steel-jacketed type K thermocouple in one of the boron nitride blocks, or a bare type K thermocouple clamped between the boron nitride blocks with the sample. Thermocouple temperature was measured with an Omega model 670 readout. Measurements at 77, 195, 273, and 373 K were verified by placing the thermocouple in liquid N_2, dry ice, ice water, and boiling water, respectively. The accuracy of the temperature measurement was estimated to be ±1 K over the entire temperature range.

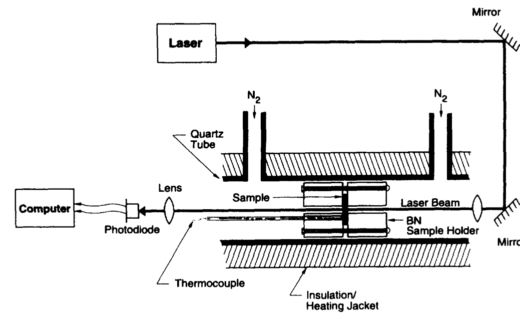

FIG. 1. Schematic diagram of experimental apparatus.

Measurements above room temperature were obtained by placing the sample holder at the center of a quartz tube furnace that was purged with nitrogen at atmospheric pressure to prevent oxidation of the samples. The infrared beam from a laser passed down the center of the tube furnace through the semiconductor sample at normal incidence, $\theta=0°$ (Fig. 1). The incident beam was focused on the sample with a 50-cm focal length lens. The temperature of the furnace was slowly increased (~3 K/min) from room temperature to a predetermined maximum value under computer control, and then allowed to cool to room temperature at a similar rate. Measurements below room temperature were obtained by mounting the sample in the boron nitride block and then suspending it on thin stainless-steel rods at the bottom of a glass cold trap. The trap was placed in a Dewar flask

TABLE I. Dopant concentrations and resistivities of samples. The symbols "+" and "−" in the last four columns indicate measurements made above room temperature and below room temperature at the corresponding wavelengths. The letter "*o*" indicates that the material is opaque at these wavelengths.

Material	N (cm^{-3})	Resistivity (Ω cm)	1.15 μm	1.31 μm	1.53 μm	2.39 μm
si-Si	−	~10^4	+	+	+	
n-Si(P)	1×10^{18}	0.019	+ −	+ −	+ −	
p-Si(B)	6×10^{14}	21	+ −	+ −	+ −	+
p-Si(B)	8×10^{14}	17	+	+ −	+	
p-Si(B)	1×10^{19}	0.008	*o*	*o*	*o*	*o*
si-GaAs	−	10^7	+ −	+ −	+ −	+
si-GaAs(110)	−	10^7	+			
n-GaAs(Te)	2.5×10^{16}	0.039	+ −	+ −	+	
n-GaAs(Te)	7.1×10^{17}	0.0032	+			
n-GaAs(Te)	1.0×10^{18}	0.0022	+			
n-GaAs(Te)	2.1×10^{18}	0.0014	+		+	
n-GaAs(S)	$1-2\times10^{18}$	0.002−0.001	+		+	
p-GaAs(Zn)	~1×10^{18}	0.06	+		*o*	
si-InP(Fe)	−	> 10^6	+ −	+ −	+ −	+
n-InP(S)	$2.6-3.9\times10^{17}$	−	+			
n-InP(S)	$2-3\times10^{18}$	−	+			
n-InP(S)	$4-5\times10^{18}$	−	+ −	+ −	+ −	
n-InP(Sn)	$1-3\times10^{18}$	−	+ −			
p-InP(Zn)	4.5×10^{18}	−	+ −	−	*o*	

and slowly cooled by adding liquid nitrogen to the flask. The inside of the cold trap was purged with nitrogen to prevent condensation. In these measurements it was more convenient to detect the reflected laser beam.

Two continuous-wave helium-neon lasers (Spectra Physics model 120 at 1.15 μm and PMS model LHIR-0100-239 at 2.39 μm) and two distributed feedback (DFB) semiconductor lasers (AT&T $In_{1-x}Ga_xAs_{1-y}P_y$ active layer at 1.5295 and 1.3106 μm) were used. The 1.15-μm He-Ne laser produces radiation at two wavelengths, 1.1526 and 1.1605 μm, with a measured intensity ratio, $I_{1.1526}/I_{1.1605}=5.06$.[3] The "beat frequency" in the interferogram at 1.15 μm, introduced by the much weaker 1.1605-μm line, was easily ignored so the β values reported correspond to $\lambda=1.1526$ μm. The 2.39-μm He-Ne laser produces several wavelengths besides the strong line at 2.395 μm. The DFB lasers produce single lines. Fewer measurements were made at 2.39 μm, and only above room temperature (see Table I). At the other wavelengths, dopant dependencies were explored above and below room temperature.

The transmitted or reflected laser beam was focused on a photodiode (Si: EG&G model FND-100 at 1.15 and 1.31 μm; or Ge: Oriel Corp. model 71150 at 1.53 and 2.39 μm) with a 10-cm focal length lens. The signal from the photodiode was amplified, and logged by a personal computer. Full interferograms were recorded, but only the temperatures at which the interferogram reached maxima and minima were used in the data analysis.

III. DATA ANALYSIS AND ESTIMATION OF ERRORS

Figure 2 is a portion of an interferogram obtained for a semi-insulating (si) GaAs wafer using a 1.53-μm DFB laser. We have chosen to label the maxima in the interferogram with integer fringe numbers; the minima are labeled with half-integer fringe numbers. The first maximum observed (typically ~298 K) was labeled $F=0$,

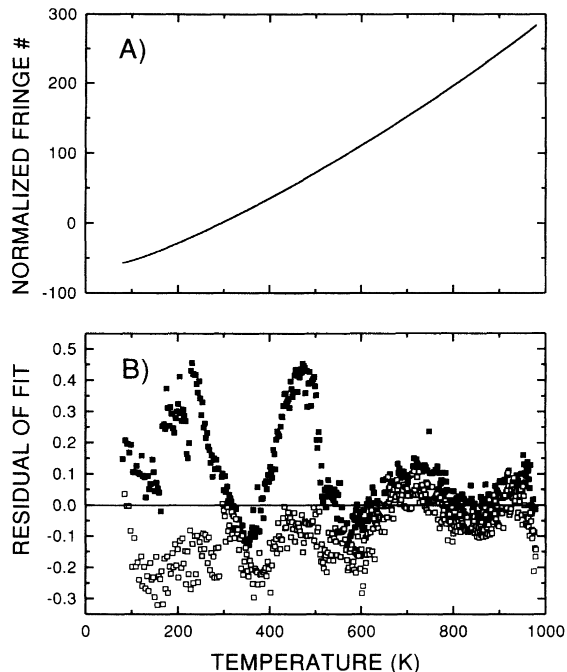

FIG. 3. (a) Representative calibration curve of fringe number versus temperature for si-GaAs at 1.530 μm. The 862 data points shown were obtained during both heating and cooling cycles in separate experiments above and below room temperature. (b) Residuals (fit to the data) of a 7th-order polynomial fit to the data in (a). ■: heating; □: cooling.

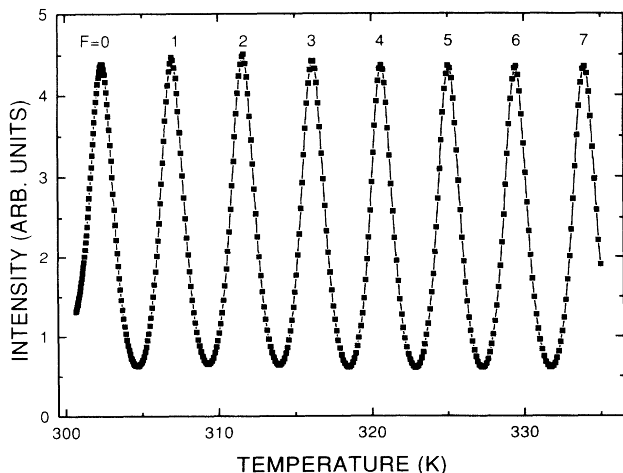

FIG. 2. Portion of an interferogram obtained while heating a si-GaAs wafer. The laser wavelength was 1.530 μm. The heating rate was ~4 K/min in this example.

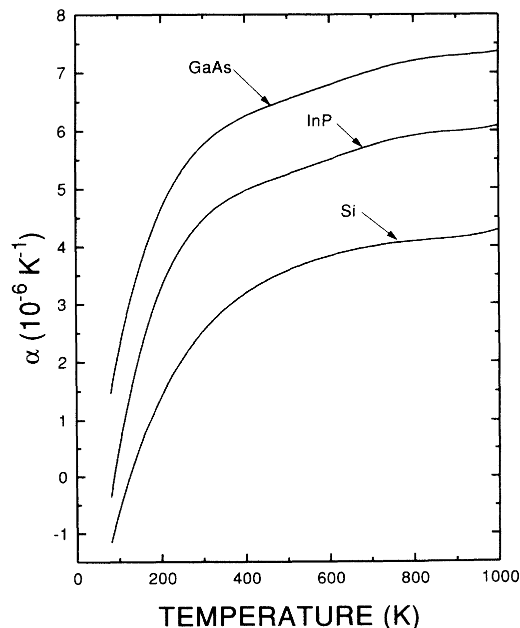

FIG. 4. Fifth-order polynomial fits to published thermal expansion data as a function of temperature for Si (Ref. 20), GaAs (Ref. 21), and InP (Ref. 22). The InP curve above room temperature was obtained by extrapolation as described in the text.

TABLE II. Refractive index at 293.2 K for Si, GaAs, and InP as a function of wavelength. Temperature corrections have been applied for GaAs and InP where $n(\lambda)$ expressions were reported for 300 and 298 K, respectively, using Eq. (6).

Sample	1.15 μm	1.31 μm	1.53 μm	2.39 μm	Reference
Si	3.5317	3.5038	3.4794	3.4415	17
GaAs	3.4440	3.4049	3.3726	3.3255	18
InP	3.2454	3.2012	3.1669	3.1198	19

and a small phase correction, ΔF, was then applied to shift the $F=0$ fringe to $T=293.2$ K. Thus, for each interferogram a data set comprising fringe numbers and temperatures is obtained. Figure 3(a) is a calibration plot of fringe number F vs temperature for si-GaAs at 1.53 μm. The fringe numbers in Fig. 3 have been normalized to a wafer thickness of 1 mm. A polynomial expression was least-squares fitted to data such as those shown in Fig. 3(a) to obtain calibration expressions of the form

$$F(T)=h(c_0+c_1T+c_2T^2+\cdots+c_7T^7) \quad (3)$$

with $h=1$ mm. A 7th-order polynomial was chosen by increasing the order until there was no significant improvement in the appearance of a plot of residuals [see Fig. 3(b)]. Although hysteresis was minimized by using very slow heating and cooling rates, the deviation of the best fit from the data is due in part to hysteresis [compare the solid and open squares in Fig. 3(b)], especially near the temperature extrema. In some instances several independent data sets were averaged before polynomial fitting.

As Saenger and Gupta noted,[6] the sum $\alpha(T)+\beta(T)$ is given by

$$\alpha(T)+\beta(T)=(\lambda/2n_ih_i)(dF/dT) \quad (4)$$

where i refers to the initial temperature T_i of 293.2 K. The temperature coefficient of n is therefore given by

$$\beta(T)=[(\lambda/2n_ih_i)(c_1+2c_2T+3c_3T^2+\cdots+7c_7T^6)]-\alpha(T)\,. \quad (5)$$

Evaluation of Eq. (5) requires values of n (293 K) for each material and wavelength. Published dispersion relations were used to calculate n (293 K) for Si,[17] GaAs,[18] and InP,[19] at 1.15, 1.31, 1.53, and 2.39 μm. The dispersion relations for GaAs and InP were reported for $T=300$ and 298 K, respectively. A small (0.05%) temperature correction was applied for each by integrating Eq. (1):

$$n(293\text{ K})=n(T)\exp[(293-T)\beta] \quad (6)$$

assuming that $\beta=6\times10^{-5}$ K^{-1}, and is temperature independent near 300 K. The resulting values are presented in Table II.

Literature values of $\alpha(T)$ for Si (Ref. 20) and GaAs (Ref. 21) were reported as separate polynomial expressions for temperatures above and below room temperature. However, they do not join smoothly at room temperature. For this reason a set of $\alpha(T)$ values was calculated over the range 80–1000 K using the two expressions; these calculated values were then fitted with a single 5th-order polynomial over the entire temperature range. The resulting best-fit $\alpha(T)$ values are presented in Fig. 4; the coefficients a_i are presented in Table III. The rms deviations of the polynomial fits are 8.1×10^{-9} and 3.4×10^{-8} K^{-1} for Si and GaAs, negligible relative to the magnitude of $\beta(T)$.

Unfortunately, high-precision $\alpha(T)$ data are available for InP only below room temperature. Haruna and Maetena[22(a)] have reviewed the available $\alpha(T)$ data for InP, and recommend the temperature-independent experimental value of Bisaro, Merenda, and Pearsall[22(b)] for $T=298$–673 K. Based on the appearance of the $\alpha(T)$ curves for Si and GaAs this seems unreasonable. We therefore chose to "extrapolate" the data of Haruna and Maetena[22(a)] from 300 to 1000 K in a manner that would yield an $\alpha(T)$ curve with a shape similar to those of Si and GaAs. This was done by splicing on the α ($T>300$ K) values of GaAs shifted downward by 1.29×10^{-6} K^{-1}. The resulting data set was then fitted with a single polynomial yielding the curve shown in Fig. 4. The difference between this extrapolation and the experimental value of Bisaro, Merenda, and Pearsall[22(b)] at 675 K is 1×10^{-6} K^{-1}. If the data of Bisaro, Merenda, and Pearsall[22(b)] are accurate, the extrapolation would incur, at most, a 2% error in the value of β (675 K) obtained from the interferometric measurements.

The $\beta(T)$ values obtained using Eq. (5) were fitted with a 7th-order polynomial to present the results and to pro-

TABLE III. Coefficients of the polynomial expressions for $\alpha(T)$: $\alpha(T)=a_0+a_1T+a_2T^2+a_3T^3+a_4T^4+a_5T^5$. Units of coefficients a_i: $K^{-(i+1)}$, e.g., for GaAs $a_2=-1.973\times10^{-10}$ K^{-3}.

Sample	a_0 1E-006	a_1 1E-008	a_2 1E-010	a_3 1E-013	a_4 1E-016	a_5 1E-020
Si	−3.884	4.397	−1.141	1.657	−1.264	3.910
GaAs	−2.386	6.446	−1.973	3.091	−2.368	7.033
InP	−4.876	7.625	−2.411	3.865	−3.019	9.131

TABLE IV. Coefficients of the polynomial fits to $\beta(T)$: $\beta(T)=b_0+b_1T+b_2T^2+b_3T^3+b_4T^4+b_5T^5+b_6T^6$. Units of coefficient b_i: $K^{-(i+1)}$, e.g., for Si at 1.53 μm $b_2=-3.72908\times10^{-9}$ K^{-3}.

Sample	λ (μm)	T range (K)	b_0 1E-005	b_1 1E-007	b_2 1E-009	b_3 1E-011	b_4 1E-014	b_5 1E-017	b_6 1E-021	rms deviation 1E-011
Si	1.15	85–520	−0.6176	1.586 32	2.563 42	−1.774 11	4.722 21	−5.700 88	25.8917	8.1
Si	1.31	85–830	−3.6137	8.650 85	−3.837 12	1.005 56	−1.498 40	1.180 78	−3.805 52	9.2
Si	1.53	85–920	−3.7239	8.614 35	−3.729 08	0.922 78	−1.270 65	0.910 77	−2.641 53	9.9
Si	2.39	295–920	−4.9739	8.914 62	−3.479 69	0.713 30	−0.720 36	0.300 47	−0.214 32	31.6
GaAs	1.15	85–890	−3.5526	13.7297	−7.295 77	2.050 15	−3.047 29	2.279 25	−6.638 20	20.9
GaAs	1.31	85–890	−3.0106	12.0132	−6.099 34	1.641 98	−2.351 18	1.706 34	−4.909 60	15.3
GaAs	1.53	85–920	−3.0585	12.0335	−6.441 95	1.819 78	−2.720 18	2.046 56	−6.085 64	20.0
GaAs	2.39	295–940	2.4978	1.672 69	−0.145 11	−0.010 97	0.236 92	−0.007 04	0.0	10.5
InP	1.15	85–780	−5.7062	16.7675	−9.995 93	3.208 48	−5.525 41	4.833 70	−16.6754	20.4
InP	1.31	85–890	3.5081	−1.361 66	2.859 55	−1.263 15	2.578 66	−2.521 08	9.584 15	8.3
InP	1.53	85–910	−3.6944	11.7540	−6.258 38	1.794 68	−2.785 29	2.213 04	−7.033 60	14.7
InP	2.39	295–930	5.6006	−0.685 58	0.311 83	−0.043 46	0.030 21	−0.009 14	0.0	16.6

vide a convenient expression for $\beta(T)$. The polynomial coefficients are presented in Table IV. Sources of error in $\beta(T)$ values calculated using the polynomials in Table IV are: laser wavelength, n (293 K), wafer thickness, measurement of $F(T)$, and polynomial fitting errors [both $F(T)$ and $\beta(T)$ fits]. Of these, the combined uncertainty due to n (293 K), λ, and h is negligible ($<1\%$). Likewise, because $\alpha(T)$ is small compared to $\beta(T)$ its small uncertainty can be neglected. Even in the worst case, InP at high temperature, it should contribute $<2\%$ uncertainty in $\beta(T)$. Most of the error in the "raw" $\beta(T)$ values seems to stem from the use of polynomials to represent the $F(T)$ data. Polynomial fitting was done to smooth the $F(T)$ data before differentiation. Two other analysis procedures [segmented cubic spline fits to $F(T)$ or pointwise differentiation of the raw $F(T)$ data followed by smoothing] were explored in an effort to avoid polynomial fitting; neither was visibly better than using polynomials. One shortcoming of polynomial fits is shown in Fig. 3(b); even with a 7th-order polynomial the residuals are not distributed randomly, although much of the deviation is due to hysteresis, as discussed above. High-order polynomials also deviate near the ends of the fitting range. To demonstrate the reproducibility of the interferometric measurements and data-analysis procedure we used, Fig. 5 shows four dF/dT curves obtained above room temperature for Si at 1.31 μm. The reproducibility is excellent except near the ends of the temperature range. The temperature ranges in Table IV have been truncated to minimize polynomial fitting artifacts. The coefficients in Table IV are reported to six digits to limit roundoff errors; they yield $\beta(T)$ values that are identical to four digits to those computed with double precision coefficients. Values of $\beta(T)$ calculated using the coefficients in Table IV have an estimated uncertainty of $\pm5\%$ within the reported temperature range. If necessary, extrapolation outside the reported temperature range should be done graphically; the polynomials are unreliable outside the reported temperature range.

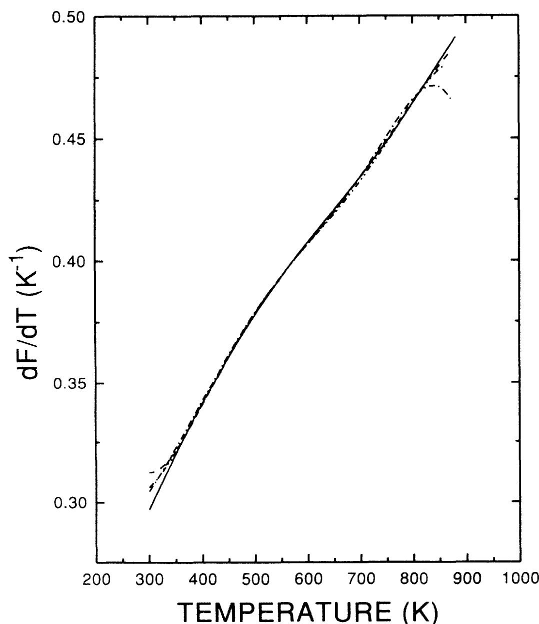

FIG. 5. First derivative plots of four polynomial fits to calibration data sets obtained above room temperature for Si at 1.31 μm.

IV. RESULTS

A. Si

Figure 6 presents $\beta(T)$ for Si at $\lambda=1.15$, 1.31, 1.53, and 2.39 μm, calculated using the polynomials in Table IV. Note that $\beta(T)$ increases strongly with T below ~250 K, and more gradually above ~250 K. In this respect $\beta(T)$ is similar to $\alpha(T)$ (compare Figs. 4 and 6). At all temperatures, $\beta(T)$ decreases with increasing wavelength. No dependence ($<1.0\%$) on doping type was found for the samples listed in Table I.

The dispersion of β (298 K) for Si in the near IR is shown in Fig. 7. Our results show a decrease of $\beta(T)$ with increasing wavelength similar to that found by Lukes,[23] however his results are systematically ~8%

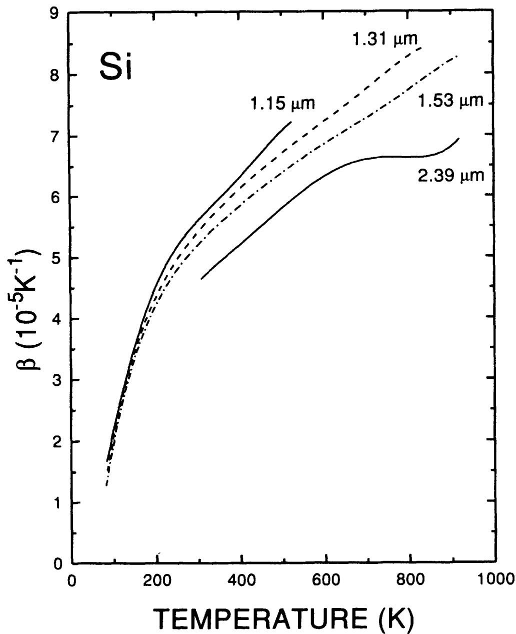

FIG. 6. Fitted values of $\beta(T)$ (from the coefficients in Table IV) of Si at 1.15, 1.31, 1.53, and 2.39 μm.

higher than ours. The dashed line in Fig. 7 is obtained from Li's recommended values of n and dn/dT.[1] Li's recommendation, which was largely based on the results of Lukes, agrees more closely with our results. Our close agreement with Li's recommendation confirms the accuracy of the interferometric method and our data-analysis procedure. Also shown in Fig. 7 is the experimental "long-wavelength limit" of β_∞ (298 K)$=4.3\times10^{-5}$,

$$\beta_\infty=(1/n_\infty)(dn_\infty/dT) \quad (7)$$

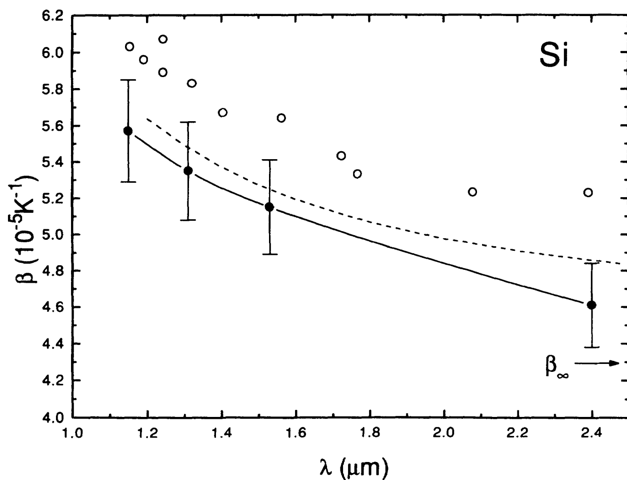

FIG. 7. Dispersion of β (298 K) for Si in the near IR. ●: This work. The smooth curve connecting the points is a spline fit. The error bars represent ±5% uncertainty. ○: Measurements by Lukes (Ref. 23). — — —: Recommendation of Li (Ref. 1). The long-wavelength limit β_∞ is from Refs. 23 and 24.

the average of values measured by Lukes[23] and Cardona, Paul, and Brooks.[24]

B. GaAs

Figure 8 presents $\beta(T)$ for GaAs at $\lambda=1.15$, 1.31, 1.53, and 2.39 μm, calculated using the polynomials in Table IV. The shape of the curve obtained at 1.15 μm suggests three significant contributions to $\beta(T)$. Below ~200 K $\beta(T)$ increases rapidly with T, approaching a plateau; this behavior is similar to that of Si at low T. An inflection point near 500 K signals the onset of another mechanism that contributes noticeably at $T>700$ K. This contribution is more obvious, and occurs at lower T, at 1.15 μm than at longer wavelengths. As with Si, no dependence (<1%) was found on doping type or level for the samples given in Table I.

The dispersion of $\beta(T)$ for GaAs in the near IR is shown in Fig. 9. As expected $d\beta(T)/d\lambda$ decreases with increasing wavelength. Cardona found β (298 K)$=4.5\pm0.2\times10^{-5}$ K^{-1} over the wavelength range 5–20 μm, and assigned this value to β_∞.[25] This value is indicated in Fig. 9.

C. InP

Figure 10 presents $\beta(T)$ for InP at $\lambda=1.15$, 1.31, 1.53, and 2.39 μm, calculated using the polynomials in Table IV. The shapes of the curves are similar to those obtained for GaAs. The low-temperature results at 1.31 μm are likely in error, i.e., the 1.31-μm curve is not expected to cross the 1.15-μm curve, as is observed near 100 K. Accordingly, a slightly more accurate value for β at 1.31 μm could be obtained by interpolation between the 1.15- and 1.53-μm curves, than from the polynomial presented

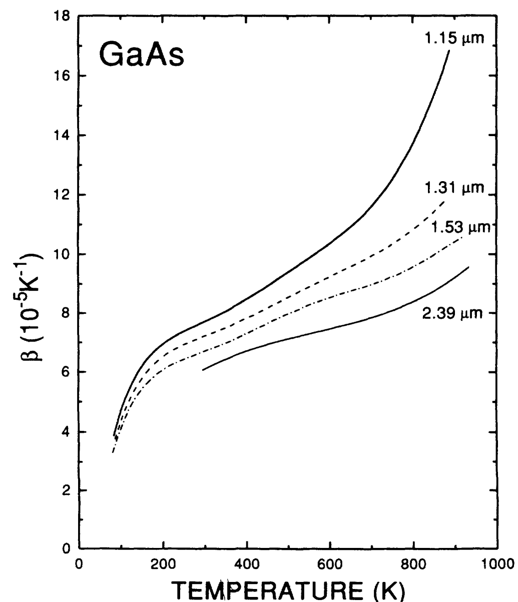

FIG. 8. Fitted values of $\beta(T)$ (from coefficients in Table IV) of GaAs at 1.15, 1.31, 1.53, and 2.39 μm.

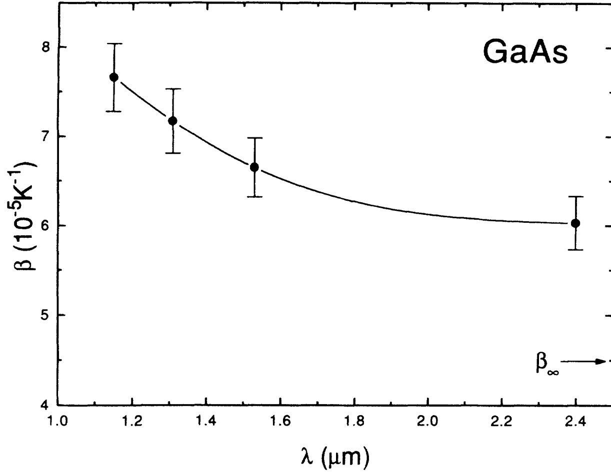

FIG. 9. Dispersion of β (298 K) for GaAs in the near IR. The smooth curve connecting the points is a spline fit. The error bars represent ±5% uncertainty.

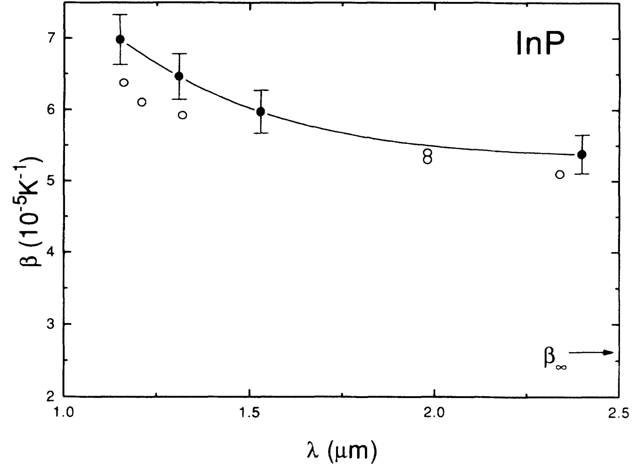

FIG. 11. Dispersion of β (298 K) for InP in the near IR. ●: This work. The smooth curve connecting the points is a spline fit. The error bars represent ±5% uncertainty. ○: Bogdanov, Prokopenko, and Yaskov (Ref. 26).

in Table IV. Consistent with the results for Si and GaAs, no dependence was found on doping type for the samples given in Table I.

The dispersion of $\beta(T)$ in the near IR is shown in Fig. 11. Agreement with the results of Bogdanov, Prokopenko, and Yaskov[26] is found to be very good, within ~8%. The value of β_∞ (298 K)$=2.7\times10^{-5}$ indicated in Fig. 11 is obtained from Cardona.[25]

Comparisons with Si reveal the importance of direct-band-gap excitation to $\beta(T)$ in GaAs and InP. $\beta(T)$ increases as the photon energy $E_{h\nu}$ is tuned toward the band-gap energy E_g at constant T. This effect is shown more dramatically by the results of Bogdanov, Prokopenko, and Yaskov because their measurements extend to shorter wavelength.[26] Equivalently, at the shortest wavelength studied (1.15 μm) a dramatic increase in $\beta(T)$ is observed at high temperature for both GaAs and InP. Because E_g decreases linearly with increasing T above 100–200 K, increasing the temperature effectively tunes E_g toward the laser photon energy, $E_{h\nu}=1.08$ eV. In both cases we find a resonance enhancement of $\beta(T)$ as the threshold for excitation across the lowest direct energy band gap is approached. This effect is discussed in more detail below.

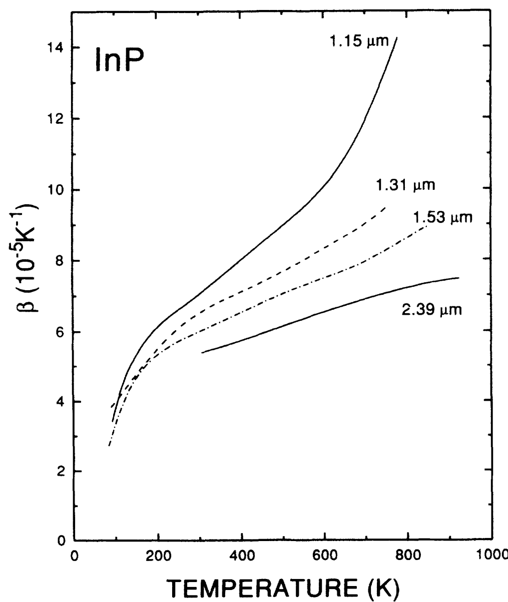

FIG. 10. Fitted values of $\beta(T)$ (from coefficients in Table IV) of InP at 1.15, 1.31, 1.53, and 2.39 μm.

V. DISCUSSION

Several theoretical investigations of the dependence of the refractive index on energy and temperature have been reported,[27–29] however, in none of these cases was the temperature dependence of β determined. We will now extend these approaches and determine this dependence, to further understand the mechanisms responsible for the observed behavior of β.

At wavelengths corresponding to energies below E_g, absorption is negligible and the index of refraction is simply the square root of the real part of the complex dielectric constant $\varepsilon_1(E,T)$,

$$n(E,T)=\sqrt{\varepsilon_1(E,T)}\ , \tag{8}$$

where E is the energy in eV. Campi and Papuzza[29] have derived an expression for $\varepsilon_1(E,T)$,

$$\varepsilon_1(E,T)=1+\frac{\eta(T)}{\pi}\left[\tfrac{1}{2}[E_{\lim}(T)^4-E_g(T)^4]+[E_{\lim}(T)^2-E_g(T)^2]E^2+\ln\left|\frac{E_{\lim}(T)^2-E^2}{E_g(T)^2-E^2}\right|E^4\right]\ , \tag{9}$$

where $E_g(T)$ is the lowest *direct* energy gap. $E_g(T)$ decreases with increasing temperature due to electron-phonon interactions, with smaller contributions from thermal expansion. Several semiempirical expressions have been given for the semiconductors considered here. We used the relationship reported by Varshni[30]

$$E_g(T)=E_g(0)-\frac{A_g T^2}{B_g+T} , \quad (10)$$

where the constants A_g and B_g are given in Table V.

Campi and Papuzza have derived *ab initio* expressions that can be used to obtain $\eta(T)$ and $E_{\lim}(T)$,[29]

$$\frac{\pi}{2}\left[\frac{4\pi e^2}{m_e}\right] n_e(E_{vl}) \left[\frac{\rho(T)N_A}{M_{av}}\right] = \frac{1}{6}\eta(T)[E_{\lim}(T)^6-E_g(T)^6] , \quad (11)$$

$$\varepsilon_1(0,T)=1+\frac{1}{2\pi}\eta(T)[E_{\lim}(T)^4-E_g(T)^4] , \quad (12)$$

where e is the elementary charge (4.803×10^{-10} $\mathrm{cm^{3/2}\,g^{1/2}\,s^{-1}}$), m_e is the rest mass of the electron (9.109×10^{-28} g), and N_A is Avagadro's number. M_{av} is the average atomic mass (g/mol) and for single-element semiconductors is simply the atomic weight. For binary compound semiconductors it is the molecular weight divided by 2. The dependence of the density $\rho(T)$ ($\mathrm{g\,cm^{-3}}$) on temperature is simply determined from the volume expansion:

$$\frac{1}{V}\frac{dV}{dT}=3\alpha(T) . \quad (13)$$

In Eq. (12), $\varepsilon_1(0,T)$ is the low-energy dielectric constant, and is given by[28,29]

$$\varepsilon_1(0,T)=1+D\left[\frac{E_p(T)}{E_{av}(T)}\right]^2 , \quad (14)$$

where $E_p(T)$ is the free-electron plasma energy and $E_{av}(T)$ is the average interband separation. D adds contributions by d electrons and is not expected to depend strongly on temperature.[28]

The quantity $n_e(E_{v1})$, given in Table V, is an effective density, representing the fraction of valence electrons participating in electronic transitions up to E_{v1}, an energy defined as the boundary between the valence region and the energy-loss region.[29] Since at E_{v1}, $n_e(E_{v1})$ is asymptotically approaching $4D$ (it reaches this value at the free-electron plasma energy),[29] and the quantities affecting $n_e(E_{v1})$ and E_{v1} depend only weakly on temperature, we ignored the slight temperature dependence of $n_e(E_{v1})$.

Yu and Cardona have equated $E_{av}(T)$ with the so-called Penn gap,[39] and derived an expression for its temperature dependence:[28]

$$\frac{1}{E_{av}(T)}\frac{dE_{av}(T)}{dT}=-\frac{3\hbar|\mathbf{g}(111)(T)|^2}{kT^2M_{av}}F(\theta_D/T) -2.4\alpha\left[\frac{E_h(T)}{E_{av}(T)}\right]^2 , \quad (15)$$

where k is the Boltzmann constant (1.3805×10^{-16} $\mathrm{erg\,K^{-1}}$), $\hbar=1.054\times10^{-27}$ erg s, and $\mathbf{g}(111)(T)$ is a reciprocal-lattice vector of length[40]

$$|\mathbf{g}(111)(T)|=2\pi\sqrt{3}/a(T) . \quad (16)$$

The lattice constant $a(T)$ varies with temperature in accordance with Eq. (2). In Eq. (15), θ_D is the Debye temperature. This parameter is derived in the Debye model approximation to the phonon density of states spectrum from atomic displacement measurements or calculations (i.e., Debye-Waller factors), and is usually represented as θ_M. Debye temperatures derived from atomic displacement are typically 5–20 % lower and much less temperature dependent ($<\sim2\%$ between 85 and 1000 K) than those derived from heat capacity data. The values for θ_M given in Table V were substituted for θ_D in Eq. (15).

The function $F(\theta_D/T)$ is an integral that has been evaluated and tabulated by Bensen and Gill.[41] In Eq. (15) the quantity $E_h(T)$ is the homopolar energy gap. It is related to the $E_{av}(T)$ and E_C, the heteropolar energy gap, by the relationship[34,42]

$$E_h(T)=\sqrt{E_{av}(T)^2-E_C^2} . \quad (17)$$

Yu and Cardona argue that the temperature dependence of E_C can be ignored with a corresponding small error in the computation of β.[28] Room-temperature values of E_C from the work of Van Vechten[34] are given in Table V.

The free-electron plasma energy (eV) is given by[29]

$$E_p(T)=6.241\times10^{11}\hbar\left[\frac{16\pi\rho(T)N_A e^2}{m_e M_{av}}\right]^{1/2} . \quad (18)$$

The factor 6.241×10^{11} converts ergs to eV.

TABLE V. Parameters used in the calculation of β. $E_g(0)$, A_g, and B_g from Refs. 31, 32, and 33 for Si, GaAs, and InP, respectively. D, E_{av}, and E_C from Ref. 34. Lattice constant, a, from Ref. 28. $n_e(E_{v1})$ from Ref. 29. θ_M for Si from the average of values in Refs. 35 and 36. θ_M for GaAs from the average of values of 295 K (Ref. 37), and values of 270 and 275 K derived from calculated and experimental Debye-Waller B factors reported in Ref. 38. θ_M for InP from the average of values of 400 K (Ref. 37), and the value of 240 K derived from calculated Debye-Waller B factors reported in Ref. 38.

Material	$E_g(0)$ (eV)	A_g (eV/K)	B_g (K)	ρ ($\mathrm{g/cm^3}$)	D	E_{av} (eV)	E_C (eV)	a (Bohr radius)	$n_e(E_{v1})$	θ_M (K)
Si	3.35	3.5×10^{-4}	580	2.33	1.00	4.8	0.0	10.26	2.71	540
GaAs	1.519	5.40×10^{-4}	204	5.333	1.08	5.2	2.9	10.68	2.87	280
InP	1.432	4.1×10^{-4}	136	4.787	1.00	5.2	3.4	11.09	2.61	320

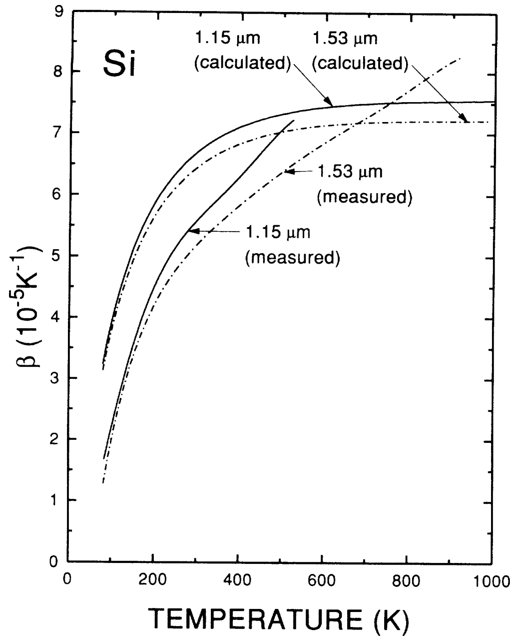

FIG. 12. $\beta(\lambda,T)$ for Si at $\lambda=1.15$ and 1.53 μm, computed from Eqs. (8)–(18), along with the experimental values from Fig. 6.

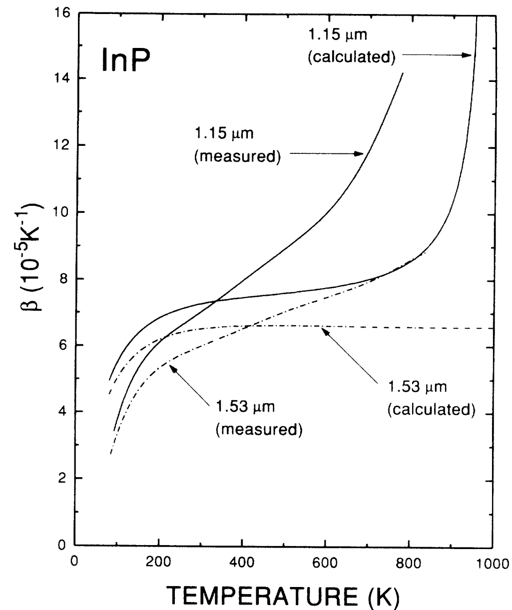

FIG. 14. $\beta(\lambda,T)$ for InP at $\lambda=1.15$ and 1.53 μm, computed from Eqs. (8)–(18), along with the experimental values from Fig. 10.

The dependence of β on temperature and energy was obtained from the above expressions, and the parameters given in Table V. The computed β values for Si, GaAs, and InP are presented in Figures 12, 13, and 14. For Si and GaAs, the agreement between experiment and theory is good, given the approximations in the model and the fact that there are no adjustable parameters. The model provides an excellent reproduction of the sharp increase in β between 85 and 250 K, although it overestimates the absolute value of β. Between 300 and 700 K, the calculated β are within 20% of the measured values, although $d\beta/dT$ over this temperature region is larger than calculated. The low temperature rise in β is due primarily to thermal expansion and its effects on the density and lattice constant, which in turn decreases the average energy gap and free-electron plasma frequency. Near room temperature, the thermal expansion coefficient becomes less strongly dependent on temperature (Fig. 4) and β correspondingly becomes less temperature dependent. Above 700 K, the rapid increase in β for GaAs at 1.15 μm is caused by the lowering of the energy of the lowest direct band gap to near resonance with the laser wavelength. The theory qualitatively reproduces this trend, however, the measured onset is much more gradual than predicted by theory.

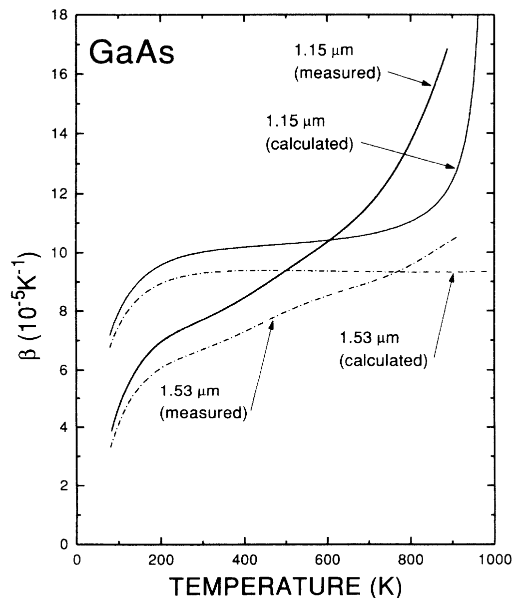

FIG. 13. $\beta(\lambda,T)$ for GaAs at $\lambda=1.15$ and 1.53 μm, computed from Eqs. (8)–(18), along with the experimental values from Fig. 8.

For Si, β does not exhibit a rapid increase at 1.15 μm and high temperature. The theory correctly reproduces this lack of an increase because the first direct energy gap of Si is much higher in energy. The lowest, indirect gap (not included in the theory) does not have a large enough oscillator strength to significantly affect β.

For InP (Fig. 14), the absolute values predicted by the theory are in good agreement with experiment at intermediate temperatures. It should be noted, however, that the absolute values of $\beta(T)$ calculated from theory are uncertain within 50% due to the large uncertainty in θ_M for InP. The theory also predicts the qualitative behavior at low temperature and at high temperature for $\lambda=1.15$ μm. However, the theory underestimates $d\beta/dT$ between 300 and 700 K, and like GaAs, it predicts too sharp an increase in β as the first direct band gap is approached.

VI. SUMMARY

Infrared laser interferometry was used to obtain accurate values of $\beta(T)$ for Si, GaAs, and InP at $\lambda=1.15$, 1.31, 1.53, and 2.39 μm. Polynomial expressions yielding $\beta(T)$ values with an estimated uncertainty of 5% are reported. Where comparison with previous work is possible, agreement within 5–10% is found. Because GaAs and InP have direct band gaps, there is a strong resonance enhancement in $\beta(T)$ as the fundamental absorption edge is approached. This is observed as $E_{h\nu}$ approaches E_g or by increasing T, which effectively tunes E_g toward $E_{h\nu}$. A considerable increase ($\sim 5\times$) in the sensitivity of interferometric thermometry of these materials could be realized, albeit at the cost of reduced temperature range, by taking advantage of this resonance enhancement. The indirect-band-gap excitation of Si has relatively little effect on $\beta(T)$.

The absolute values and temperature dependences of β are reasonably well reproduced by existing theory. The calculated values of β are not, however, of sufficient accuracy to apply interferometric thermometry with acceptable accuracy, hence the experimental measurements were necessary. The measured values of β presented in this study are of sufficient accuracy to allow theories to be further refined and tested.

ACKNOWLEDGMENTS

We thank E. Lory, T. R. Hayes, R. F. Karlicek, and D. L. Coblentz for providing substrates and S. Pearton for help in performing Hall effect measurements. We thank PMS Inc. for loaning us a 2.39-μm He-Ne laser.

---

*Present address: Hoechst Celanese Research Division, 86 Morris Ave., Summit, NJ 07901.

†Present address: Princeton High School, Princeton, NJ 08544.

[1] H. H. Li, J. Phys. Chem. Ref. Data **9**, 561 (1980).

[2] J. A. McCaulley and V. M. Donnelly, J. Chem. Phys. **91**, 4330 (1989).

[3] V. M. Donnelly and J. A. McCaulley, J. Vac. Sci. Technol. A **8**, 84 (1990).

[4] V. M. Donnelly and J. A. McCaulley, U.S. Patent No. 5,229,303, 20 July 1993.

[5] H. Sankur and W. Gunning, Appl. Phys. Lett. **56**, 2651 (1990).

[6] K. L. Saenger and J. Gupta, Appl. Opt. **30**, 1221 (1991).

[7] D. Hacman, Optik **28**, 115 (1968).

[8] R. A. Bond, S. Dzioba, and H. M. Naguib, J. Vac. Sci. Technol. **18**, 335 (1981).

[9] V. M. Donnelly, J. Vac. Sci. Technol. A **11**, 2393 (1993).

[10] K. L. Saenger, F. Tong, J. S. Logan, and W. M. Holber, Rev. Sci. Instrum. **63**, 3862 (1992).

[11] V. M. Donnelly, Appl. Phys. Lett. **63**, 1396 (1993).

[12] V. M. Donnelly and J. A. McCaulley, Surf. Sci. **238**, 34 (1990).

[13] T. R. Hayes, P. A. Heimann, V. M. Donnelly, and K. E. Strege, Appl. Phys. Lett. **57**, 2817 (1990).

[14] V. M. Donnelly, D. E. Ibbotson, and C.-P. Chang, J. Vac. Sci. Technol. A **10**, 1060 (1992).

[15] V. R. McCrary, V. M. Donnelly, S. G. Napholtz, T. R. Hayes, P. S. Davisson, and D. C. Bruno, J. Cryst. Growth **125**, 320 (1992).

[16] J. A. McCaulley, M. Vernon, I. Taha, and V. M. Donnelly (unpublished).

[17] M. Herzberger and C. D. Salzberg, J. Opt. Soc. Am. **52**, 420 (1962).

[18] J. S. Blakemore, J. Appl. Phys. **53**, R123 (1982); (see page R147).

[19] G. D. Pettit and W. J. Turner, J. Appl. Phys. **36**, 2081 (1965).

[20] Y. S. Touloukian, R. K. Kirby, R. E. Taylor, and T. Y. R. Lee, *Thermophysical Properties of Matter, Vol. 13, Thermal Expansion* (Plenum, New York, 1977), pp. 155–156.

[21] J. S. Blakemore, J. Appl. Phys. **53**, R123 (1982); (see page R133).

[22] (a) K. Haruna and H. Maeta, in *Properties of Indium Phosphide* (The Institution of Electrical Engineers, New York, 1991), pp. 16 and 17; (b) R. Bisaro, P. Merenda, and T. P. Pearsall, Appl. Phys. Lett. **34**, 100 (1979).

[23] F. Lukes, Czech. J. Phys. B **10**, 317 (1960).

[24] M. Cardona, W. Paul, and H. Brooks, J. Phys. Chem. Solids **8**, 204 (1959).

[25] M. Cardona (unpublished).

[26] V. B. Bogdanov, V. T. Prokopenko, and D. D. Yaskov, Opt. Spectrosc. (USSR) **60**, 68 (1986).

[27] F. Stern, Phys. Rev. **133**, A1653 (1964).

[28] P. Y. Yu and M. Cardona, Phys. Rev. B **2**, 3193 (1970).

[29] D. Campi and C. Papuzza, J. Appl. Phys. **57**, 1305 (1985).

[30] Y. P. Varshni, Physica **34**, 149 (1967).

[31] P. Lautenschlager, M. Garriga, L. Vina, and M. Cardona, Phys. Rev. B **36**, 4821 (1987).

[32] J. S. Blakemore, J. Appl. Phys. **53**, R123 (1982); (see page R155).

[33] Z. Hang, H. Shen, and F. H. Pollak, Solid State Commun. **73**, 15 (1990).

[34] J. A. Van Vechten, Phys. Rev. **182**, 891 (1969).

[35] B. W. Batterman and D. R. Chipman, Phys. Rev. **127**, 690 (1962).

[36] P. J. E. Aldred and M. Hart, Proc. R. Soc. London Ser. A **332**, 239 (1973).

[37] N. N. Sirota, in *Semiconductors and Semimetals,* edited by R. K. Willardson and A. C. Beer (Academic, New York, 1968), Vol. 4, p. 131.

[38] J. S. Reid, Acta. Crystall. A **39**, 1 (1983).

[39] D. R. Penn, Phys. Rev. **128**, 2093 (1962).

[40] J. M. Ziman, *The Principles of the Theory of Solids* (Cambridge University Press, New York, 1969), p. 14.

[41] G. C. Benson and E. K. Gill, Can. J. Phys. **44**, 674 (1966).

[42] J. C. Phillips, Phys. Rev. Lett. **20**, 550 (1968).